Increased motion and travel, rather than stable docking, characterize the last moments before secretory granule fusion

Vadim E. Degtyar*, Miriam W. Allersma*, Daniel Axelrod†‡, and Ronald W. Holz*§

Departments of *Pharmacology, †Physics, and ‡Biophysics, University of Michigan, Ann Arbor, MI 48104-0632

Edited by Charles F. Stevens, Salk Institute for Biological Studies, La Jolla, CA, and approved August 20, 2007 (received for review June 8, 2007)

The state of secretory granules immediately before fusion with the plasma membrane is unknown, although the granules are generally assumed to be stably bound (docked). We had previously developed methods using total internal reflection fluorescence microscopy and image analysis to determine the position of chromaffin granules immediately adjacent to the plasma membrane with high precision, often to within ≈10 nm, or <5% of the granule diameter (300 nm). These distances are of the dimensions of large proteins and are comparable with the unitary step sizes of molecular motors. Here we demonstrate with quantitative measures of granule travel in the plane parallel to the plasma membrane that secretory granules change position within several hundred milliseconds of nicotinic agonist-induced fusion. Furthermore, just before fusion, granules frequently move to areas that they have rarely visited. The movement of granules to new areas is most evident for granules that fuse later during the stimulus. The movement may increase the probability of productive interactions of the granule with the plasma membrane or may reflect the pull of molecular interactions between the granule and the plasma membrane that are part of the fusion process. Thus, instead of being stably docked before exocytosis, granules undergo molecular-scale motions and travel immediately preceding the fusion event.

chromaffin cells | exocytosis | granule motion | total internal reflection fluorescence microscopy

The last moments of a secretory granule before fusion with the plasma membrane have been the subject of intense investigation and much speculation. Electron micrographs of endocrine cells, including chromaffin cells (1–3), show close apposition of secretory granules to the plasma membrane. Granules can fuse within 100 ms of a Ca^{2+} stimulus (4, 5), with rapid secretion lasting for 0.5–1 s and slower, sustained secretion occurring over many seconds to minutes (5, 6). From detailed kinetic analyses of secretion from chromaffin cells (7), it has been postulated that granules are stably bound to the plasma membrane, where they undergo priming (6, 8) and soluble NSF attachment receptor (SNARE) interactions (9) before they are competent to undergo exocytosis.

Another view of events comes from studies using total internal reflection fluorescence microscopy (TIRFM) to investigate granule behavior immediately adjacent to the plasma membrane in chromaffin cells. A common finding in these studies is that most granules adjacent to the plasma membrane are highly restricted in their motion as if tethered or caged (3, 10–14), rarely moving their diameter over tens of seconds to several minutes. Secretion occurs from these granules. Although restricted, the small jittering motions are regulated by Ca^{2+} and ATP (14) and by various proteins (15–18). Granules undergo exocytosis during nicotinic agonist stimulation without apparent biased movement closer toward the glass interface (14).

We had previously developed methods using TIRFM and image analysis to determine the position of chromaffin granules with high precision, often to within ≈10 nm, or <5% of the granule diameter (300 nm) (13). These distances are of the dimensions of large proteins and are comparable with the unitary step sizes of molecular motors. Now we have devised quantitative measures of granule travel in the plane parallel to the plasma membrane. We demonstrate that granules destined to fuse during nicotinic stimulation change position (tens of nanometer displacements) rather than becoming immobilized within a few hundred milliseconds of fusion. Furthermore, just before fusion, granules frequently move to areas that they have rarely visited, indicating an enabling role for granule motion in fusion.

Results

To determine the relationship between the restricted travel of secretory granules and fusion, chromaffin cells were stimulated with the nicotinic agonist 1,1-dimethyl-4-phenylpiperazinium (DMPP), which causes Ca^{2+} influx and secretion. The distinct signature of fusion obtained with VAMP-GFP-labeled granules (increased brightness and rapid spreading of the fluorescence) permitted timing of the beginning of fusion events to within 0.1–0.2 s (13). Granules were followed at 10 Hz before and during stimulation until fusion. Two representative tracks are shown in Fig. 1 *A* and *B*. Before stimulation (black tracks), granules were dithering within confined regions of ≈30-nm diameter. Upon stimulation (red tracks), the granules increased their motion and moved tens of nanometers before fusion at 3 s (Fig. 1*A*) or several 100 nm before fusion at 14 s (Fig. 1*B*). In each case the last position before fusion (Xs in blue circles) was isolated from most of the previous track. To understand these motions better, the paths of large numbers of fusing and nonfusing granules were analyzed.

We first measured individual *R* motions (in the plane parallel to the glass interface) of fusing granules as a function of time before fusion. Because there is considerable variability of the motion of individual granules, ΔR was expressed for each granule relative to its average ΔR before stimulation. Complicating the analysis is the fact that granules fused at various times (2–16 s) after the beginning of stimulation with DMPP. Tracks for 72 granules were aligned at the frame just before fusion, and relative ΔR for individual granules before fusion were averaged for each aligned frame (Fig. 1*C Upper*). ΔR substantially increased within 1 s of fusion, with a maximum twice that of the prestimulation value at the time of fusion. Such a large increase in ΔR was specific for granules undergoing secretion. Nonfusing

Author contributions: M.W.A., D.A., and R.W.H. designed research; M.W.A. performed research; D.A. contributed new reagents/analytic tools; V.E.D., D.A., and R.W.H. analyzed data; and R.W.H. wrote the paper.

The authors declare no conflict of interest.

This article is a PNAS Direct Submission.

Abbreviations: DMPP, 1,1-dimethyl-4-phenylpiperazinium; SNARE, soluble NSF receptor; TIRFM, total internal reflection fluorescence microscopy; VAMP, vesicle-associated membrane protein.

§To whom correspondence should be addressed at: 2301 MSRB III, Department of Pharmacology, University of Michigan Medical School, Ann Arbor, MI 48109-0632. E-mail: holz@umich.edu.

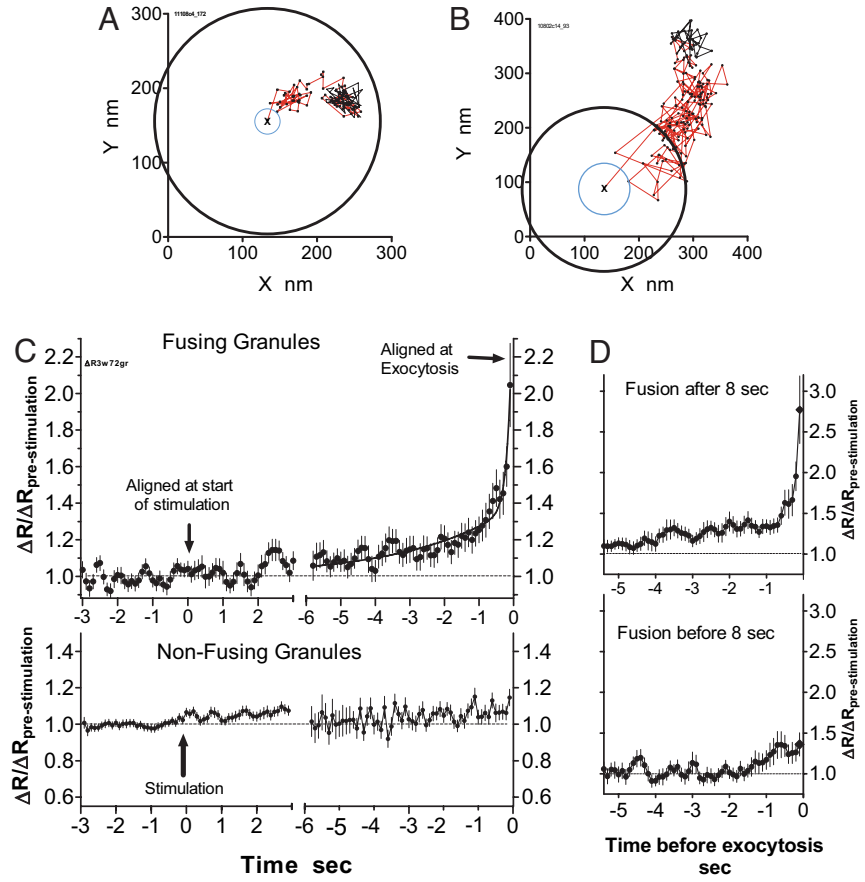

Fig. 1. Granules increase their motions just before exocytosis. (*A* and *B*) Tracks of two granules before stimulation (black path) and during stimulation with DMPP (red path) until fusion (marked with X). The large black circles represent a 300-nm granule centered on the last position before fusion. The blue circles in *A* and *B* are used in the visit density analysis (see *Methods*) and have radii of 17 and 47 nm, respectively. (*C*) (*Upper*) The motion of granules destined to fuse during stimulation was expressed relative to the average motion before stimulation, $\Delta R/\Delta R_{prestimulation}$. Paths of 72 granules immediately before fusion were aligned at the time of fusion (right side) or at the time of stimulation (left side). The average ± SEM of $\Delta R_{prestimulation}$ was 25.3 ± 1.1 nm. The time course was subjected to a sliding three-position smoothing algorithm. The last motion before fusion was not smoothed. There was an increase in motion in the last few hundred milliseconds of fusion, with the motion during the last 100 ms of fusion being twice that of the prestimulation motions. (*Lower*) The same analysis was performed on nonfusing granules. Nonfusing granules were selected from the same cells as those in *Upper*. Their motions were aligned during stimulation to the average time at which granules were fusing in the same cell. Nonfusing granules did not substantially increase their motion when neighboring granules are fusing. (*D*) Time courses of increases in $\Delta R/\Delta R_{prestimulation}$ for 35 granules that fused after 8 s of stimulation (*Upper*) and for 37 granules that fused during the first 8 s of stimulation (*Lower*).

granules in the same cells analyzed at the same time as their fusing neighbors did not display this increased motion (Fig. 1*C Lower*). In a previous study we found that average ΔR averaged over the last second before fusion increased by 32% (recalculated from ref. 14). The current analysis with 10 times the temporal resolution revealed a larger (100%) increase in motion within the last 200 ms of fusion (Fig. 1*C Upper*).

We asked whether the increase in motion before fusion occurred similarly for 37 granules that fused early (within 8 s) and 35 granules that fused later during the stimulation. The increase in motion was observed in both groups of granules, but to our surprise, we found that the increase in motion was larger for granules that fused later (Fig. 1*D Upper*). Motions of these granules increased 175% within a few hundred milliseconds of fusion, whereas the motions of the earlier secreting granules increased by 40% (Fig. 1*D Lower*). The largest increases in motion occurred in the later-fusing granules within 200 ms of fusion (Fig. 1*D Upper*), with smaller increases in motion earlier.

The increase in frame-to-frame motions of the granules could reflect increased jittering of the granules without granules traveling to new regions. Alternatively, the granules could be traveling away from their previous positions. These possibilities were investigated by measuring the maximum distance between any two positions that a granule visited in 1 s. Granules that fused after 8 s of stimulation had a strong tendency for increased travel in the last second before fusion compared with travel during 1 s before stimulation (Fig. 2*A*). The median of the maximum distances increased from 56 to 114 nm (35 granules, $P < 0.0001$, Mann–Whitney test). There was also a significant, albeit smaller, tendency for granules that fused during the first 8 s of stimulation to increase their maximum travel in the second before fusion (Fig. 2*B*); the median value increased from 62 to 76 nm (37 granules, $P < 0.05$, Mann–Whitney test). Significant changes were not observed for nonfusing granules analyzed at the same time as their fusing neighbors. The median of the maximum travel of 277 nonfusing granules was 53 nm and 56 nm, before and during stimulation (difference not significant, Fig. 2*C*).

The maximum distance traveled in last second before fusion and during 1 s before stimulation were compared for each granule (Fig. 2*D*). The distance traveled increased for virtually every granule that fused after 8 s (34 of 35 granules, filled circles). The expanded range of travel began within seconds before exocytosis (Fig. 2*F*). The tendency was less for granules that fused more rapidly (25 of 37 granules, open circles) and was

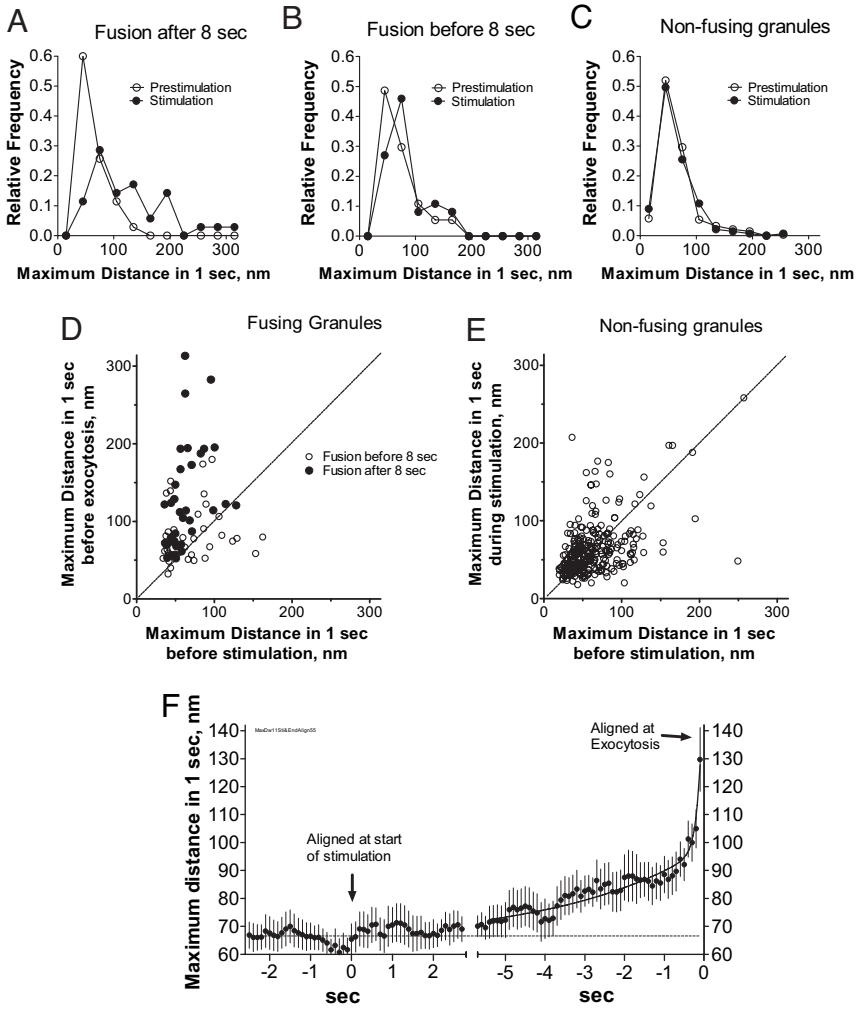

Fig. 2. Fusing granules increase their travel immediately before exocytosis. The maximum distances traveled in 1 s before stimulation and within 1 s of fusion were determined for granules that fused after 8 s of stimulation ($n = 35$; *A*) and before 8 s of stimulation ($n = 37$; *B*). Data are presented as a histogram with a bin size of 30 nm in *A* and *B*. (*C*) Nonfusing granules. The same analysis as in *A* and *B* was performed on 273 nonfusing granules with alignment during stimulation at the average time at which granules were fusing in the same cell. (*D*) A granule-by-granule comparison of the maximal distances traveled by granules immediately before fusion and before stimulation with DMPP. Open and filled circles correspond to granules that fused before and after 8 sec, respectively. (*E*) Nonfusing granules. The same analysis as in *D* was performed on nonfusing granules aligned during stimulation to the average time at which granules were fusing in the same cell. The dotted lines in *C* and *D* are at a 45° angle with the axes. (*F*) Time course of the extent of travel in 1 s. Granule paths were aligned as in Fig. 1*C*. Maximum distances traveled in sliding 1-s (10 frame) windows were averaged for 55 granules that fused after 6 s of stimulation.

not evident for nonfusing granules analyzed in the same cells and at the same time as their fusing neighbors (Fig. 2*E*). However, there was a small increase in maximum distance traveled in 1 s for nonfusing granules (15%) during extended times of stimulation (>8 s, data not shown), consistent with a global change in granule travel (14).

If the probability of fusion is independent of position and purely stochastic, then granules would tend to fuse in areas where they spend the most time. However, inspection of a large number of granule tracks including those in Fig. 1 *A* and *B* suggested that this was not the case. Not only was there an increase in motion, there was also a tendency for the last position before fusion to be separated by tens of nanometers from positions that the granule had visited previously. This observation was quantified by counting for each position the number of times in the track that the granule was found within a specified radius of that position ("visit density"; for full description, see *Methods*). The visit density of the last position before fusion was compared with the average visit density of all of the previous positions in the track. Because of the large granule-to-granule differences in motion, the radius used for each granule was the standard deviation of its frame-to-frame motions in the X or Y direction during the time interval (for rationale, see *Methods*). Thus, a granule with large average motions was assigned a large visit radius, whereas a granule with small average motions was assigned a small visit radius.

As suspected, there was a strong tendency for granules to move into a new area immediately before fusion. This tendency was most evident for late-fusing granules (Fig. 3*A*, filled circles). Fifty-eight percent of these fusion events occurred to granules that had suddenly moved to an area that they had rarely or never visited before (zero to two visits, bin size 3). In contrast, during the rest of the track (29 positions), granules tended to visit areas that they had occupied before (Fig. 3*A*, open circles). Only 12% of the time did granules move to a position that had been visited twice or less. When the motions of the same granules before stimulation were analyzed in the same way, there was no difference between the visit density of the last position and the 29 previous positions (Fig. 3*B*). The frequency of zero to two previous visits to the same area for the last position was only

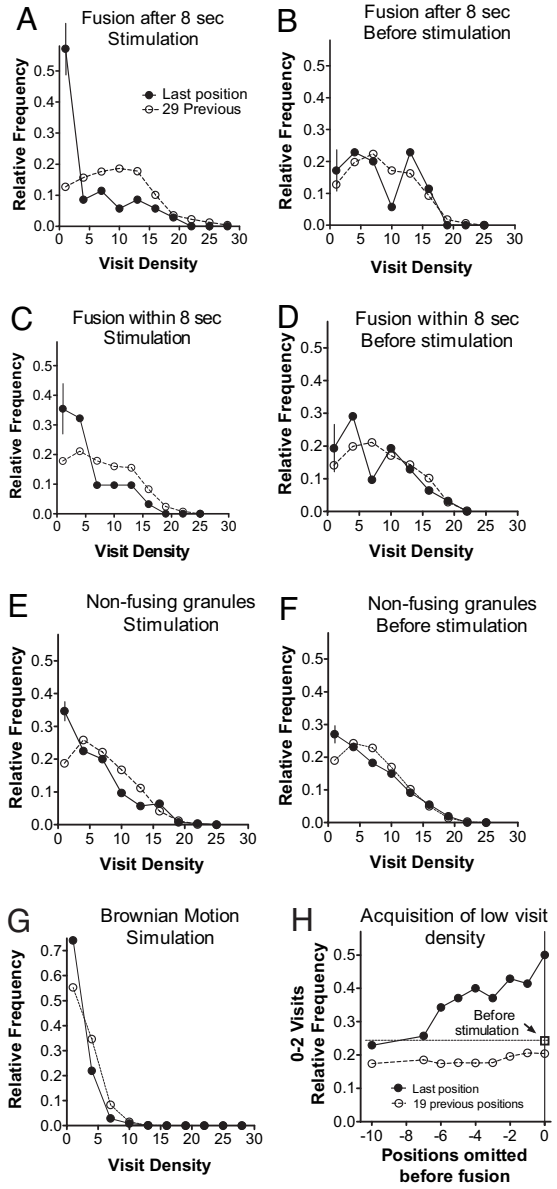

Fig. 3. Granules tend to move to new positions immediately before exocytosis. The number of times a granule was within a small radius of each position was determined (visit density). For every granule position within 3 s of fusion or during a 3-s interval before stimulation, the distances from all other 29 positions (*A–F*) or 19 positions (*H*) were calculated (10-Hz frame rate). The frame-to-frame standard deviation of ΔX or ΔY of each granule during the 3-s interval was used as the visit radius (see *Methods*). In practice, the average visit radii for the different populations of granules were 18–30 nm. The visit density histogram of the last position (filled circles) and the combined histogram of the visit densities of the previous positions are presented (open circles). (*A* and *B*) Granules that fused after the 8 s of stimulation. The histograms of the visit densities of the last position in *A* and *B* were significantly different (35 granule tracks, medians 2 and 5, respectively; $P < 0.005$, Mann–Whitney). (*C* and *D*) Granules that fused before 8 s of stimulation. The histogram of the visit densities of the last positions in *C* and *D* were significantly different (37 granule tracks, medians 3 and 6, respectively; $P = 0.035$, Mann–Whitney). (*E* and *F*) Nonfusing granules. Paths were aligned during stimulation to the average time at which neighboring granules fused in the same cell. There were 280 and 307 tracks in *E* and *F*, respectively. Medians of last positions were both 5. In *A–F*, the error bars in the lowest visit density of the last positions are based on a binomial distribution of either being or not being in that bin. The visit density of the last position in *A* was significantly different from that in *C* and *E* ($P < 0.0001$). (*G*) Visit density simulation for a granule undergoing Brownian motion. The probabilities were determined from 1,000 simulations of a 30-position track. The visit radius, as in the analysis of actual granule travel, was set to be equal to the standard deviation of random set of ΔX (or ΔY) picked from a Gaussian distribution. The square of the standard deviation of ΔX (or ΔY) is proportional to the diffusion coefficient of the simulated path. (*H*) Acquisition of low visit densities. One to 10 of the last positions before exocytosis were omitted, and the visit densities of the previous 20 positions were analyzed for the combination of early- and late-fusing granules. The relative frequencies of zero to two visits were plotted. The frequency of zero to two visits of the last position of a 20-position sequence before stimulation for the same granules was also determined (open square and dotted line).

17%. The tendency of granules to increase their travel into new areas immediately before fusion was significantly greater ($P < 0.0001$) for granules that fused after 8 s (Fig. 3*A*) than for granules that fused within the first 8 s (Fig. 3*C*) and for nonfusing granules analyzed at the same time as their fusing neighbors (Fig. 3*E*).

We compared the behavior of actual granules with that of a hypothetical granule undergoing simple Brownian motion. As with the analysis of the visit density of actual granules, the visit radius used for the simulation was set equal to the standard deviation of the step-to-step motions in the *X* or *Y* direction. The analyses demonstrate that the tendency of actual, late-fusing granules to move into a new area in its last position before fusion is similar to a hypothetical granule undergoing Brownian motion (compare filled circles in Fig. 3 *A* and *G* at the lowest visit density). However, the average of the previous 29 positions is much more highly restricted compared with Brownian motion (compare open circles in Fig. 3 *A–F* with those in Fig. 3*G*). Thus, granules immediately before fusion travel as if they have become less restricted.

The tendency to travel to new areas begins several hundred milliseconds before fusion, which is demonstrated by sequentially omitting from the analysis the 10 last positions before exocytosis (Fig. 3*H*). The analysis includes both early- and late-fusing granules. As positions were eliminated before exocytosis, the previous 20 positions were analyzed. The tendency for the granule to move into new areas progressively increases only within 0.7 s of fusion. Before this time, the likelihood of the granule being in an area that had been visited only zero to two times was similar to that of the last position of a 20-position sequence before stimulation (open square and dotted line). Pure Brownian motion simulation with a constant, single diffusion coefficient would not show this progressive increase. This comparison of actual versus simulated motion supports the notion that there is a tendency for granules to become less restricted before fusion.

In a previous study, we found that exocytosis occurred without biased motion toward the glass interface within 400–200 ms of fusion (14). In the present work, the analysis was extended back to 10 s before fusion. Again, no significant (>5 nm) bias of frame-to-frame motion toward the glass interface was detected, either for the early- or late-fusing granules (data not shown).

Discussion

The results from this work demonstrate an unexpected and significant increase of travel of secretory granules parallel to the plasma membrane shortly before fusion, often to regions not previously visited. Because neighboring, nonfusing granules analyzed at the same time do not have this tendency, the movement is likely to reflect important steps that make fusion imminent. The results are contrary to the notion of a necessary, long-lived docked state as a prelude to fusion.

There are at least two possible explanations for the observation of greater travel preceding fusion. One explanation is statistical. Some granules are favorably positioned at the time of stimulation to interact with key proteins or lipids, thus allowing

fusion to occur relatively quickly with little travel. These granules may be part of the rapidly releasable pool detected after flash photolysis of caged Ca^{2+} (7). However, many granules are not in a favorable location for fusion. For such granules, sampling the plasma membrane in virgin territory rather than in domains that the granule had already visited unproductively increases the probability of subsequent fusion. Indeed, the greater tendency of late-fusing granules to travel to new areas in the last few hundred milliseconds before fusion supports this notion. The increased travel could reflect the action of molecular motors (e.g., myosin Va or myosin II) (19, 20) or sudden granule untethering (consistent with the Brownian motion simulation; Fig. 3*G*).

A second explanation is that the increased motion reflects part of the mechanism of the fusion process itself. Lateral forces from asymmetrical arrangement of protein interactions between the granule and the plasma membrane may cause travel. For example, the zippering of a single SNARE complex could cause motion of ≈10 nm (21); successive formation of several quaternary SNARE complexes may move granules greater distances. Relatively small increases in motion could reflect these molecular interactions. The travel that these processes reflect could be part of a Ca^{2+}-dependent priming step that precedes fusion (6, 22).

These explanations are not mutually exclusive. For example, granules in unfavorable locations may only fuse if they increase their travel, perhaps because of untethering. Upon arrival at a fusion competent site, granules are subject to additional motion because of interactions with plasma membrane proteins, including t-SNARES or with plasma membrane lipids such as phosphatidylinositol (4,5)-bisphosphate (23, 24).

There is general agreement that granules close to the plasma membrane move much less than expected for a sphere in a high-viscous medium of the cytoplasm. Caging and tethering have been suggested by us and others as explanations. However, it is possible that a diffusion (Brownian motion) model based on the actual small frame-to-frame motions is sufficient to explain the range of travel. A simulation of Brownian motion indicates that even taking into account low granule mobility, the average travel of granules is much more spatially limited than predicted for Brownian motion (Fig. 3). On the other hand, the increased travel of late-fusing granules immediately before fusion approaches travel of a Brownian particle. This increased travel could reflect the partial release of caged or tethered granules before fusion.

Lower temporal resolution studies support our conclusion that molecular scale motions and travel often immediately precede granule fusion. Ng *et al*. (25) and Burke *et al*. (26) demonstrated that increased granule motion is well correlated with increased probability of fusion in PC12 cell growth cones (25, 26) and at the *Drosophila* neuromuscular junction (27, 28). In the latter, Ca^{2+}/calmodulin and calmodulin kinase II were implicated in increased motion and secretion (27). Furthermore, immobilization of granules before fusion was not detected in *Drosophila* neuromuscular junction (28), hippocampal neuron growth cones (29), or PC12 growth cones (25, 26, 30). Vesicle motion is probably also important for fast release in at least some neurons. Fast, tonic neurotransmitter release at the ribbon synapse in the inner hair cell neuron requires continuous and rapid vesicle replenishment from remote regions in the cell with vesicle residence times at release sites of tens of milliseconds or less (31). Thus, our finding that motion and travel, rather than stable docking, can immediately precede and may facilitate fusion is likely to be relevant to other secretory cells.

Although granules did not have a bias toward travel toward the glass interface from 10 s to 200 ms of fusion, we had previously found that there was a significant tendency for granules to brighten in the last 100 ms before fusion (14), consistent with movement toward the plasma membrane. However, an increase in granule intensity could also reflect the capturing of the beginning of a fusion event because of the effect of increased pH on EGFP fluorescence before diffusion of VAMP-GFP into the plasma membrane. Indeed, the tendency for granules to brighten initially is anticipated because it would reflect the formation of a narrow fusion pore responsible for slow catecholamine release or "feet" that sometimes precede amperometric spikes of catecholamine release by 100 ms or less (32, 33). It is, therefore, uncertain whether granules, on the average, move toward the glass interface within 100 ms of fusion. However, the tendency for increased granule travel parallel to the glass interface before fusion begins many hundreds of milliseconds before fusion and before possible biased motion toward the glass interface. If granules are not undergoing biased motion toward the glass interface within 200 ms of fusion, they may be already close enough to the plasma membrane to fuse, or they could be fusing with plasma membrane invaginations.

Finally, it should be noted that bovine chromaffin cells used in this work are primary, nondividing cells. The characteristics of relatively slow motions of chromaffin granules (average short-term diffusion coefficient 3×10^{-12} cm^2/s) and the rarity of appearance of new granules in the evanescent field (12) are similar to those of insulin granules in unstimulated, healthy rat and human pancreatic islet beta cells (average short-term diffusion coefficient, 5×10^{-12} cm^2/s) (34). In contrast, granule mobility is often much greater in continuous cells lines that display regulated exocytosis. For example, granules in PC12 cells (from a rat chromaffin cell tumor line) and INS-1 cells (from an insulin-secreting tumor line) have short-term diffusion coefficients ≈7-fold (11) and 100-fold (35) greater, respectively, than in the primary cells. Similarly, granules in mouse embryonic chromaffin cells show much greater mobility, with 20% having residence times of <10 s in the evanescent field (17) compared with <1% in adult bovine chromaffin cells (12). Thus, changes in granule motion before exocytosis may be significantly different in these continuous cell lines and embryonic cells than in fully differentiated primary cells.

Methods

Chromaffin cell preparation from bovine adrenal medulla and transient transfection were performed as described previously (36). Prismless (through-the-objective) TIRFM experiments were performed with a ×100 1.65 N.A., oil immersion objective (Olympus Corporation, Melville, NY) giving a decay constant for the evanescent field of 55 nm (14). Solution was delivered to the cells by using a positive pressure from a computer-controlled perfusion system DAD-6VM (ALA Scientific Instruments, Westbury, NY).

Granules were identified and tracked through a time sequence stack of images by using software written by the authors in Interactive Data Language (ITT Visual Information Solutions, Boulder, CO) (14). Software was written to automate the reading and analysis of multiple granule tracks.

Visit density was the measure of the tendency of the granule to remain in an area. For tracks of 20 (Fig. 3*H*) or 30 frames (Fig. 3 *A–F*), the distances between every pair of positions were calculated. The visit density of a given granule position was the number of times in the track that the granule was found within a specified radius of that position. For example, a visit density of 0 means that the granule was only in the area once in the entire track, whereas a visit density of 10 means that the granule had been located within the area 10 additional times. Picking a specific visit radius for the analysis proved difficult because of the large differences of average motions of individual granules. A fixed radius applied to the entire population of granules would give an imprecise measure of the tendency of granules to move to previously unexplored regions. For example, if the radius is small compared with the average motion of a granule, then the visit densities would be low.

Conversely, if the radius is large compared with the average motion of a granule, then the visit densities would be high. Instead, the standard deviation of ΔX or ΔY from frame to frame for each granule was used as the visit radius, which is formally equivalent to $(2D\Delta t)^{1/2}$ where D is the short-term diffusion coefficient and Δt the interframe interval. This self-adjusting parameter permitted an unbiased assessment of the uniqueness of the positions in a granule path. Its utility is shown in Fig. 1 *A* and *B*, where the radii (blue circles) were very different: 17 and 47 nm based on their motion in the last 30 frames before fusion. The visit densities of the last positions before fusion in Fig. 1 *A* and *B* were 0 and 1, respectively.

We are deeply indebted to Dr. Mary A. Bittner for carefully reading and editing the manuscript. This work was supported by National Institutes of Health Grant R01 NS38129 (to R.W.H. and D.A.).

1. Nakata T, Hirokawa N (1992) *J Neurosci* 12:2186–2197.
2. Vitale ML, Seward EP, Trifaro J-M (1995) *Neuron* 14:353–363.
3. Steyer JA, Horstman H, Almers W (1997) *Nature* 388:474–478.
4. Horrigan FT, Bookman RJ (1994) *Neuron* 13:1119–1129.
5. Voets T (2000) *Neuron* 28:537–545.
6. Bittner MA, Holz RW (1992) *J Biol Chem* 267:16219–16225.
7. Rettig J, Neher E (2002) *Science* 298:781.
8. Holz RW, Bittner MA, Peppers SC, Senter RA, Eberhard DA (1989) *J Biol Chem* 264:5412–5419.
9. Xu T, Rammner B, Margittai M, Artalejo AR, Neher E, Jahn R (1999) *Cell* 99:713–722.
10. Oheim M, Loerke D, Stuhmer W, Chow RH (1998) *Eur J Biophysics* 27:83–98.
11. Lang T, Wacker I, Wunderlich I, Rohrbach A, Giese G, Soldati T, Almers W (2000) *Biophys J* 78:2863–2877.
12. Johns LM, Levitan ES, Shelden ES, Holz RW, Axelrod D (2001) *J Cell Biol* 153:177–190.
13. Allersma MW, Wang L, Axelrod D, Holz RW (2004) *Mol Biol Cell* 15:4658–4668.
14. Allersma MW, Bittner MA, Axelrod D, Holz RW (2006) *Mol Biol Cell* 17:2424–2438.
15. Huet S, Karatekin E, Tran VS, Fanget I, Cribier S, Henry JP (2006) *Biophys J* 91:3542–3559.
16. Tsuboi T, Fukuda M (2006) *Mol Biol Cell* 17:2101–2112.
17. Toonen RF, Kochubey O, de W, Gulyas-Kovacs A, Konijnenburg B, Sorensen JB, Klingauf J, Verhage M (2006) *EMBO J* 25:3725–3737.
18. Nofal S, Becherer U, Hof D, Matti U, Rettig J (2007) *J Neurosci* 27:1386–1395.
19. Neco P, Gil A, Frances M, Viniegra S, Gutierrez LM (2002) *Biochem J* 368:405–413.
20. Rose SD, Lejen T, Casaletti L, Larson RE, Pene TD, Trifaro J-M (2003) *J Neurochem* 85:287–298.
21. Liu W, Montana V, Bai J, Chapman ER, Mohideen U, Parpura V (2006) *Biophys J* 91:744–758.
22. von Rüden L, Neher E (1993) *Science* 262:1061–1065.
23. Eberhard DA, Cooper CL, Low MG, Holz RW (1990) *Biochem J* 268: 15–25.
24. Hay JC, Fisette PL, Jenkins GH, Fukami K, Takenawa T, Anderson RA, Martin TFJ (1995) *Nature* 374:173–177.
25. Ng YK, Lu X, Gulacsi A, Han W, Saxton MJ, Levitan ES (2003) *Biophys J* 84:4127–4134.
26. Burke NV, Han W, Li D, Takimoto K, Watkins SC, Levitan ES (1997) *Neuron* 19:1095–1102.
27. Shakiryanova D, Klose MK, Zhou Y, Gu T, Deitcher DL, Atwood HL, Hewes RS, Levitan ES (2007) *J Neurosci* 27:7799–7806.
28. Shakiryanova D, Tully A, Hewes RS, Deitcher DL, Levitan ES (2005) *Nat Neurosci* 8:173–178.
29. Silverman MA, Johnson S, Gurkins D, Farmer M, Lochner JE, Rosa P, Scalettar BA (2005) *J Neurosci* 25:3095–3106.
30. Han W, Ng YK, Axelrod D, Levitan ES (1999) *Proc Natl Acad Sci USA* 96:14577–14582.
31. Griesinger CB, Richards CD, Ashmore JF (2005) *Nature* 435:212–215.
32. Zhou Z, Misler S, Chow RH (1996) *Biophys J* 70:1543–1552.
33. Chow RH, von Rüden L, Neher E (1992) *Nature* 356:60–63.
34. Michael DJ, Xiong W, Geng X, Drain P, Chow RH (2007) *Diabetes* 56:1277–1288.
35. Ivarsson R, Obermuller S, Rutter GA, Galvanovskis J, Renstrom E (2004) *Traffic* 5:750–762.
36. Wick PW, Senter RA, Parsels LA, Holz RW (1993) *J Biol Chem* 268:10983–10989.